SIMULATION OF PHYSICAL PROCESSES

Original article
DOI: https://doi.org/10.18721/JPM.18102

# A SUPERSONIC VISCOUS GAS FLOW PAST A BLUNT CYLINDRICAL BODY BOUNDED AT ITS ENDS BY PARALLEL PLATES

*E. V. Kolesnik*✉, *E. V. Babich*, *E. M. Smirnov*

Peter the Great St. Petersburg Polytechnic University, St. Petersburg, Russia

✉kolesnik_ev@mail.ru

**Abstract.** The paper presents the results of calculations of a supersonic laminar flow past a cylindrical body located between parallel horizontal walls (plates). The free-stream Mach number M = 5. Calculations were carried out for various values of the geometric factor $\chi$ defined as the ratio of the distance between the walls to the blunt diameter of the leading edge of the body, the ratio varying from 2 to infinity. Decreasing the distance between the walls was shown to lead to a shift of the separated shock closer to the streamlined body, and to an increase in the thickness of the separation region. In the case of $\chi = 2$ a nonstationary self-oscillatory flow regime characterized by strong oscillations of the separated shock wave was realized.

**Keywords:** high-speed flow, numerical simulation, internal separated flow, viscous-inviscid interaction, horseshoe vortex

**Funding:** The reported study was funded by Russian Science Foundation (Grant No. 23-29-00286).

**Citation:** Kolesnik E. V., Babich E. V., Smirnov E. M., A supersonic viscous gas flow past a blunt cylindrical body bounded at its ends by parallel plates, St. Petersburg State Polytechnical University Journal. Physics and Mathematics. 18 (1) (2025) 18–29. DOI: https://doi.org/10.18721/JPM.18102



Научная статья
УДК 519.6:533.6.011
DOI: https://doi.org/10.18721/JPM.18102

# СВЕРХЗВУКОВОЕ ОБТЕКАНИЕ ВЯЗКИМ ГАЗОМ ЗАТУПЛЕННОГО ЦИЛИНДРИЧЕСКОГО ТЕЛА, ОГРАНИЧЕННОГО С ТОРЦОВ ПАРАЛЛЕЛЬНЫМИ ПЛАСТИНАМИ

*Е. В. Колесник*✉, *Е. В. Бабич*, *Е. М. Смирнов*

Санкт-Петербургский политехнический университет Петра Великого, Санкт-Петербург, Россия

✉kolesnik_ev@mail.ru

**Аннотация.** В работе представлены результаты расчетов сверхзвукового ламинарного обтекания затупленного цилиндрического тела, расположенного между параллельными стенками (пластинами). Число Маха набегающего потока M = 5. Расчеты проведены для различных значений геометрического параметра $\chi$, определяемого как отношение расстояния между пластинами к диаметру затупления передней кромки тела и изменяемого от 2 до бесконечности. Показано, что при уменьшении расстояния между пластинами отошедший скачок уплотнения смещается ближе к обтекаемому телу, а толщина отрывной области увеличивается. В случае $\chi = 2$ реализуется нестационарный автоколебательный режим обтекания, характеризующийся сильными колебаниями отошедшего скачка уплотнения.

**Ключевые слова:** высокоскоростное течение, численное моделирование, внутреннее отрывное течение, вязко-невязкое взаимодействие, подковообразный вихрь

**Финансирование:** Исследование выполнено при финансовой поддержке Российского научного фонда (грант № 23-29-00286).

**Ссылка для цитирования:** Колесник Е. В., Бабич Е. В., Смирнов Е. М. Сверхзвуковое обтекание вязким газом затупленного цилиндрического тела, ограниченного с торцов параллельными пластинами // Научно-технические ведомости СПбГПУ. Физико-математические науки. 2025. Т. 18. № 1. С. 18–29. DOI: https://doi.org/10.18721/JPM.18102



## Introduction

Problems of supersonic flow, characterized by complex effects of viscous-inviscid interaction, are important both for many practical applications, for example, for the aerospace industry and turbomachinery, and for fundamental research. Numerous studies, both experimental and computational, consider separation phenomena in bodies streamlined by external flow (see, for example, [1–6]). A detailed review of the data obtained in recent years on the characteristics of three-dimensional flow that occurs during the interaction of a detached boundary layer with a leading-edge shock is given in [7].

There are far fewer studies on internal separation flows. The effects of the viscous-inviscid interaction play an even greater role here [8]. Deceleration of supersonic flow in channels can lead to separation of the boundary layer and the formation of a pseudo-shock [9–11]. In the case of rectangular channels, corner boundary layers can significantly affect the flow structure, even regions far from the corners [12–14]. It is also known that effects induced by unsteady phenomena play a major role in the development of separation flows in channels [8]. The internal problems of viscous-inviscid interaction, covering a wide variety of complex phenomena, are far from fully understood, requiring new research. Methods of three-dimensional numerical simulation are gaining popularity, since they allow to obtain a picture of the flow with all of its significant details.

This paper presents the procedure and results for a study of supersonic flow around an elongated cylindrical body bounded at the ends by parallel plates. We considered the influence of the relative distance between the plates on the flow structure and flow regimes, including the resulting unsteady self-oscillatory flows.

Solutions to this type of problems are essential, in particular, for design of experiments on supersonic flow around various bodies, where the bounding walls of the setup have a considerable influence on the flow [7]. Research in this direction is carried out with both pulse generators and in supersonic wind tunnels, but the flow is almost always internal in both cases.

## Problem statement and computational aspects

Fig. 1 shows the coordinate system and the computational domain for the given problem of a symmetrical cylindrical body streamlined by supersonic viscous flow of ideal gas, located between parallel plates. The dimensions of the main part of the computational domain are $L^*\times 2R\times H$, where $L^*\times 2R$ are the dimensions of the plate, $H$ is the variable distance between the plates; the remaining dimensions are fixed, including the distance $L$ from the body to the leading edge of the plate (assumed to be infinitely thin). The blunt-fin diameter $D$of body's leading edge, taken equal to 0.02 m, is used as the length scale. The simulations were performed for $L/D = 15$, $R/D = 10$, $L^*/D = 20$. The computational domain also contained a small primary section, whose length was set equal to $D$. The ratio of the distance between the plates to the blunt-fin diameter (geometric parameter $\chi = H/D$) ranged from 2 to 4; simulations were also performed for the case $\chi \to \infty$, which corresponds to the problem of external flow around a cylindrical body, traditionally considered in a region semi-bounded along the $Z$ axis.

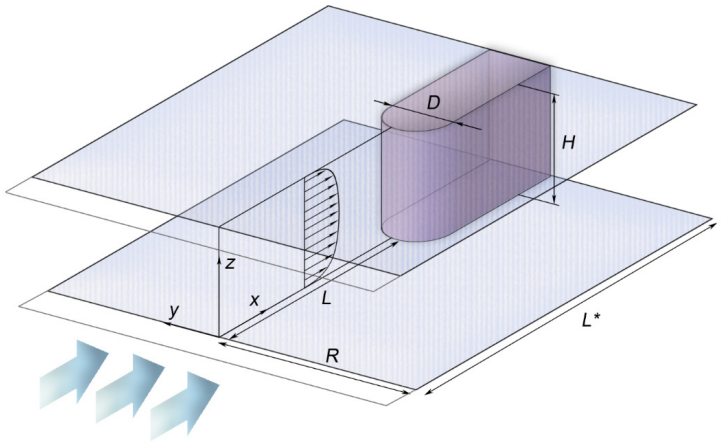


Fig. 1. Flow pattern and computational domain (sized $L^*\times 2R\times H$): $D$ is the diameter of the blunt-fin diameter of leading edge of symmetrical cylindrical body, $L$ is the distance from the body to the leading edge of the plate, $H$ is the variable distance between the plates
The arrows show the propagation direction of supersonic flow

It is assumed that the Mach number of the incident flow $M_{in} = 5$, and the unit Reynolds number $Re = 7.5\cdot 10^5$ m$^{-1}$. The total temperature of the incident flow is $T_0 = 1180$ K, the working gas is nitrogen ($\gamma = 1.4$, $C_p = 1040$ J/(kg·K)). Laminar flow occurs with these parameters (the Reynolds number, based on the given value of the blunt-fin diameter, $Re = 1.5\cdot 10^4$). The temperature dependence of viscosity is determined by the Sutherland formula. Homogeneous flow is set at the inlet boundary of the computational domain, and a no-slip condition is set on the surface of the body and plates. The surfaces of the body and plates are maintained at a constant temperature $T_w = 300$ K, with a temperature factor $T_w/T_{in} = 1.56$. Symmetry conditions are imposed on the boundaries of the primary section ($Z$ = const). Non-reflecting boundary conditions are imposed at the lateral boundaries, and a gradient condition for zero gradient of the calculated variables is imposed at the outlet.

Numerical solutions of 3D Navier–Stokes equations were obtained via the finite-volume unstructured program code SINF/FlagS, developed at Peter the Great St. Petersburg Polytechnic University.

All simulations were carried out in an unsteady formulation, the two-step method was used with a three-layer scheme for approximating the time derivative, the dimensionless time step was set equal to $\Delta t U_\infty/D = 10\cdot 3.5^{-3}$. Convective flows at the faces of the control volumes were calculated using the second-order AUSM scheme, and a quasi-one-dimensional van Albada limiter was used for preserving the solution monotonicity.

Meshes containing about 15 million cells were used for the simulations. The parameters of the computational meshes were selected based on analysis of the results obtained in [5]. A view of the mesh near the junction between the body and one of the plates is shown in Fig. 2.

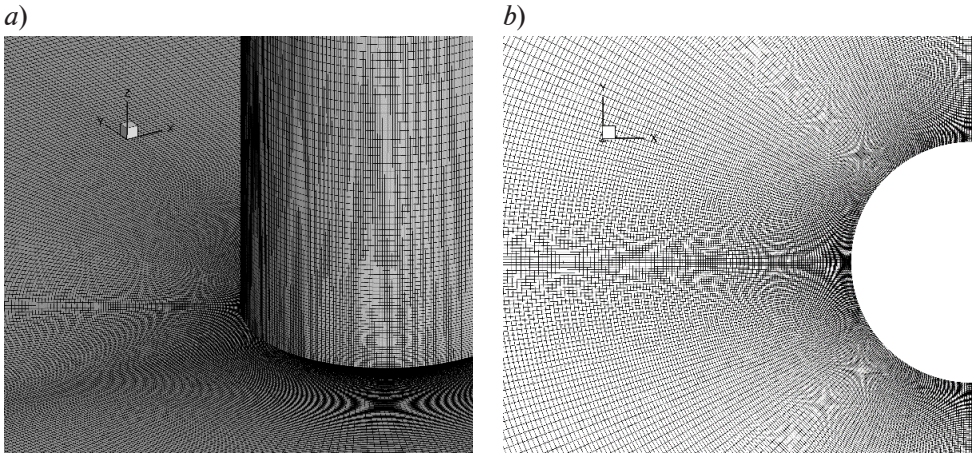


Fig. 2. 3D (*a*) and 2D(*b*) fragments of the computational mesh near the junction between cylindrical body and plate (*a*) and near one of the plates (*b*)

### Flow structure in semi-bounded region

The numerical solution obtained for the semi-bounded region ($\chi \to \infty$) corresponds to steady flow around a body symmetrical with respect to the vertical symmetry plane. The structure of the flow near the junction is given in Fig. 3, showing the streamlines and the distribution of relative pressure on the surface of the body and plate ($P_{in}$ is the freestream static pressure). The characteristics of the flow under consideration can be clearly seen: the formation of a separation region with a system of horseshoe-shaped vortices and the presence of a region with increased pressure on the surface of the body at the stagnation point.

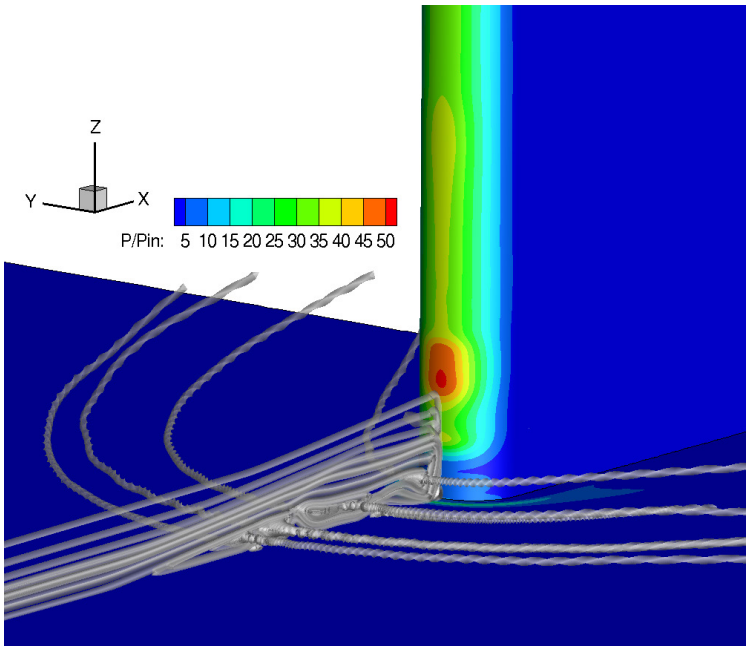


Fig. 3. Streamlines (shown in gray) and pressure distribution over the surfaces of body and plate, simulated for the case $\chi \to \infty$ (external flow around the body)

The structure of the flow in the symmetry plane is given in Fig. 4, where the fields of the Mach number and the density gradient magnitude (numerical Schlieren) are shown along with the streamline pattern. A leading-edge shock forms in front of the body, and an adverse pressure gradient leads to separation of the boundary layer. The separation region induces oblique compression waves intersecting with the leading-edge shock, bending it towards the streamlined body. Regions with supersonic velocities and local compression waves appear within the separation region, inducing secondary separation of the near-wall flow. Consequently, an extended separation region with a chain of vortex structures evolves in front of the body, each of them becoming the 'head' of a horseshoe-shaped vortex enveloping the body. Due to this flow structure, regions of non-monotonic parameter distribution appear on the surfaces of the plate and body. The latter show the presence of local maxima for pressure and Stanton number St (Fig. 5) near the junction.

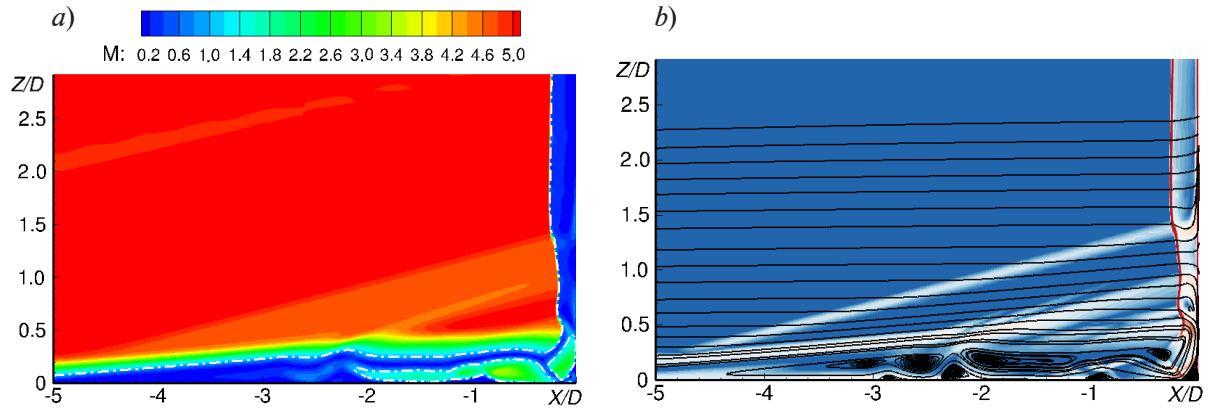


Fig. 4. Fields of Mach number (*a*) and density gradient magnitude with superimposed streamlines (*b*) in the vertical symmetry plane

The Stanton number was calculated by the formula

$$St = \frac{q_w}{\rho_{in} V_{in} C_p (T_{aw} - T_w)}, \; T_{aw} = T_{in}\left(1 + r\frac{\gamma - 1}{2} M_{in}^2\right),$$

where $q_w$ is the local heat flux; $T_{aw}$ is the 'adiabatic' temperature; $r = \sqrt{\mathrm{Pr}}$ is the recovery factor (Pr is the Prandtl number); $T_w$ is the wall temperature; $\rho_{in}$, $V_{in}$, $M_{in}$ are the freestream density, velocity, and Mach number, respectively.

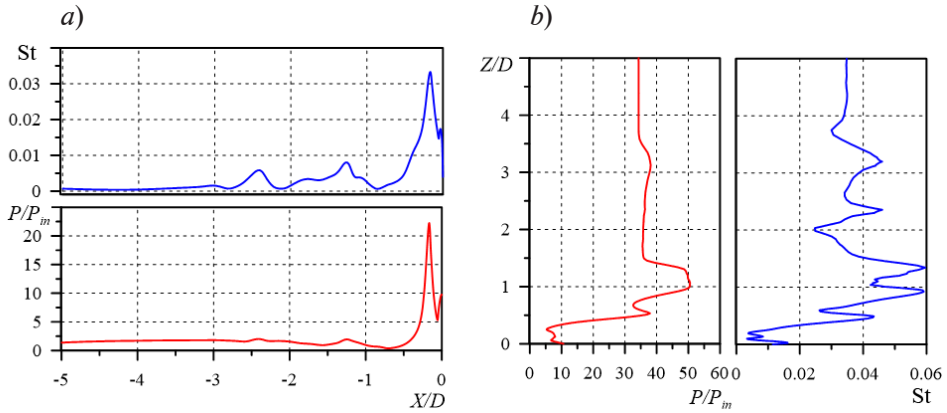


Fig. 5. Distribution of normalized pressure and Stanton number St over plate surface, along symmetry line, for $\chi \to \infty$ (*a*) and over cylindrical body along the leading edge (*b*) (see Fig. 1)

**Computational results with varying distance between bounding plates**

As noted above, steady flow occurs for $\chi \to \infty$. The flow simulated at $\chi = 4$ and 3 can be characterized as weakly unsteady: fluctuations relatively low intensity are observed in local flow parameters only near the junction between the body and the plates. When the geometric parameter is reduced to $\chi = 2$, the flow pattern becomes significantly unsteady.

Fig. 6 shows Mach number fields with superimposed streamlines in the vertical symmetry plane in front of the streamlined body (time-averaged fields are shown for unsteady regimes). In the case when $\chi = 4$, a pronounced inviscid flow core is observed in the center of the channel formed by the plates; in this case, the bow shock in the plane $Z/D = 2$ (average over $Z$) is located at almost the same distance from the body as in the case of a semi-bounded region (the difference is less than 3%). If the parameter $\chi$ is decreased to 3, the bow shock is noticeably shifted closer to the streamlined body, while the thickness of the separation region increases only slightly. In the case when $\chi = 2$, the structure of the averaged flow in the separation region is considerably different: the number of pronounced vortices is smaller and the separation region is less extensive.

Fig. 7 shows the images obtained by numerical Schlieren visualization of the flow near the plate surface (Fig. 7,*a*, instantaneous fields are shown), as well as time-averaged pressure distributions along the leading edge over the cylindrical body (the leading edge is shown in the inset to Fig. 7,*b* by a red segment). Analyzing the distributions in the range of the normalized coordinate $0 \le Z/D \le 2$, we can conclude that the shock wave patterns simulated for $\chi \to \infty$ and $\chi = 4$ have a similar appearance. In particular, in both of these cases, the pressure maximum is detected at a distance $Z/D \approx 1$ from the plate. With a further decrease in the relative distance between the plates, the regions of viscous-inviscid interaction located near the plates begin to increasingly affect the inviscid flow core, and then each other, which eventually leads to qualitative transformation of the flow. In the case when $\chi = 3$, the pressure maximum is observed in the center of the channel, while additional local maxima are observed near the walls; the bow shock in the central zone is significantly close to the body. In the case when $\chi = 2$, only one pressure maximum is observed on the distribution curve, located in the center of the channel. In general, as the distance between the plates decreases, the peak pressure value increases; in the case when $\chi = 2$, this increase is 40% of the peak value in the solution for a semi-bounded area.

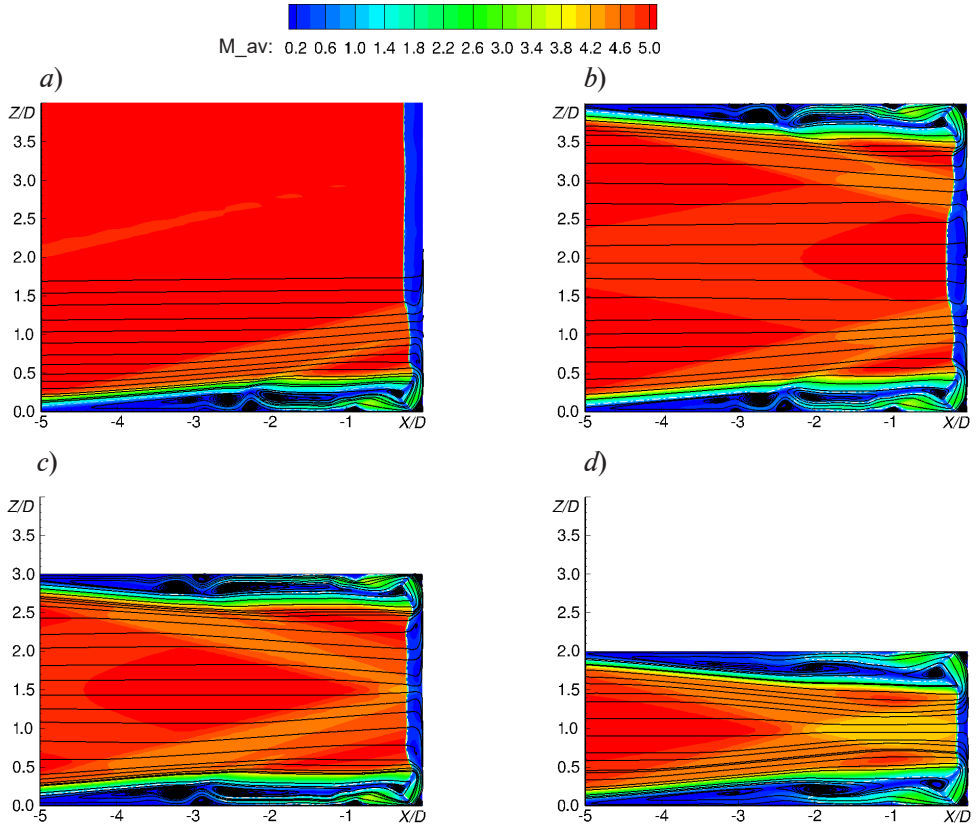


Fig. 6. Mach number fields with superimposed streamlines in vertical symmetry plane, simulated for different values of the parameter $\chi$: $\to\infty$ (*a*), 4 (*b*), 3 (*c*) and 2 (*d*)

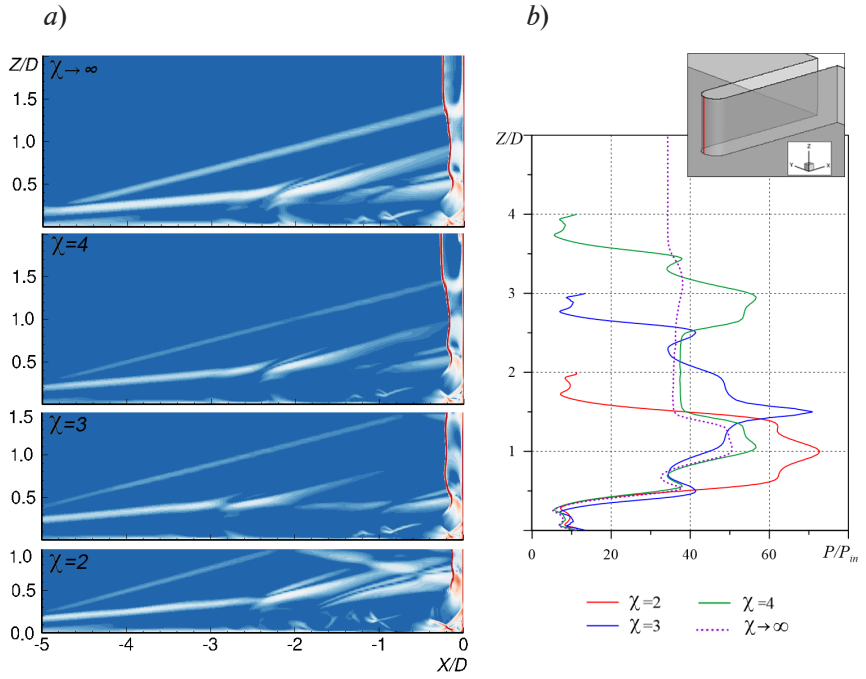


Fig. 7. Fields of density gradient magnitude in the vertical symmetry plane in front of the cylindrical body (*a*) and pressure distribution along the leading edge on the body (*b*)
The leading edge is shown in the inset by a red segment

Fig. 8 shows the computational distributions of the Stanton number over the surface of the body and over the plate (time-averaged fields are shown for unsteady regimes). As the distance between the plates decreases, the peak values of the heat flux increase. The presence of two symmetrical regions of enhanced heat transfer is clearly visible on the surface of the body in the case of a relatively large distance between the plates ($\chi = 4$). In the case when $\chi = 3$, the maximum values of the Stanton number are observed in the central zone, and additional local maxima of lower amplitude are formed near the plates. If $\chi = 2$, the region of enhanced heat transfer occupies almost the entire surface of the body along the height, while the maximum heat flux values in the horseshoe-shaped region on the surface of the plate are comparable to the peak values on the surface of the body.

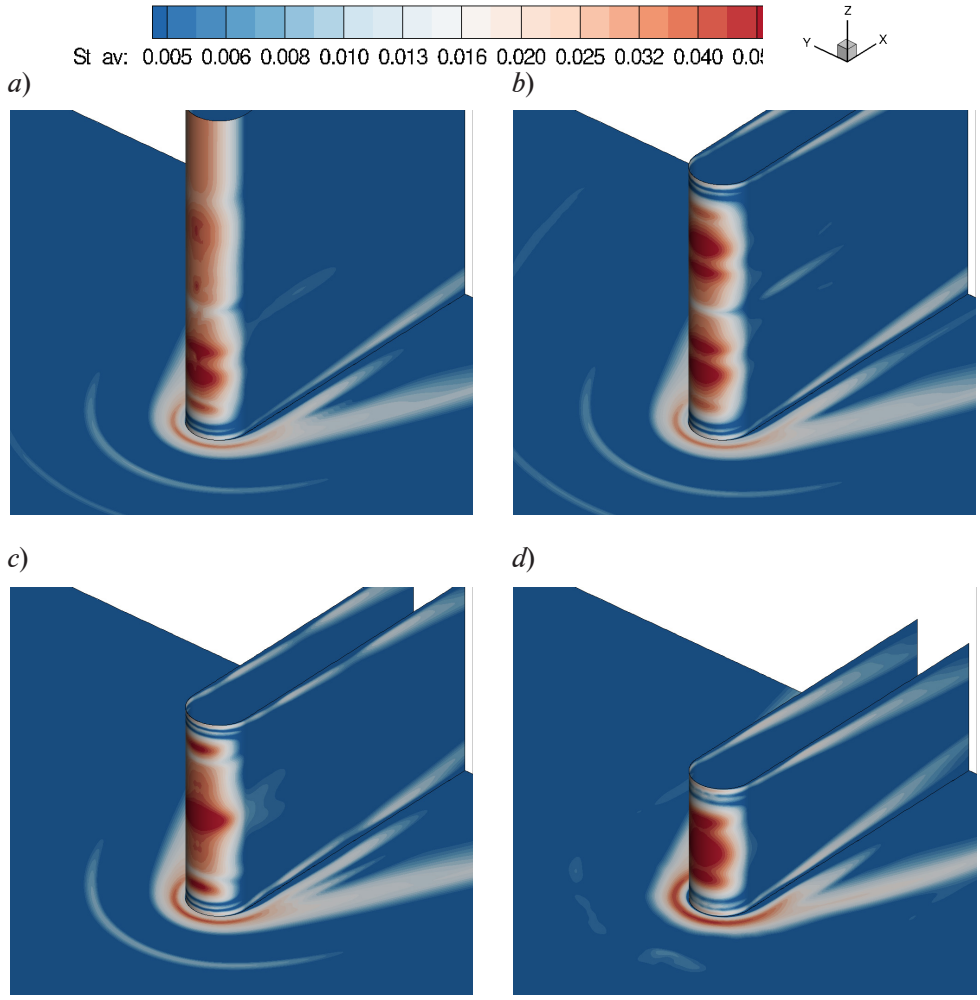


Fig. 8. Distributions of Stanton number over the surface of plate and over cylindrical body, simulated for different values of the parameter $\chi$: $\to\infty$ (*a*), 4 (*b*), 3 (*c*) and 2 (*d*)

## Characteristics of self-oscillatory flow

This section describes in more detail the computational results for the case $\chi = 2$, when significantly unsteady flow evolves (as noted above).

Fig. 9 shows the time-averaged pressure field and the field of RMS fluctuations (on a logarithmic scale) on the surfaces of the body and the plate. Significant pressure fluctuations are observed on the plate surface in the region of the local pressure maximum, with the fluctuation level of about 30% of the maximum value. Intense fluctuations are observed along the front; it should also be noted that there are regions with increased pressure fluctuations on the lateral surfaces of the body.

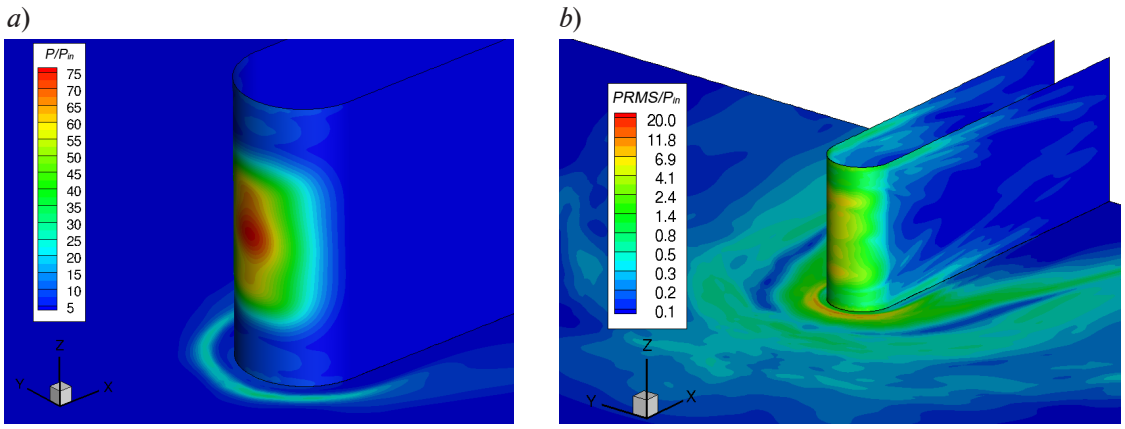


Fig. 9. Fields of average pressure (*a*) and RMS pressure fluctuations (*b*) on the surfaces of body and plate, simulated for the case $\chi = 2$

Fig. 10 shows the time dependences of pressure at several points on the surfaces of the plate and the body; points located symmetrically relative to the symmetry plane ($Z/D = 1$) are selected. If the time-averaged flow is symmetrical relative to the central plane, then the data in Fig. 10 are clear evidence for the asymmetry of the instantaneous flow fields. Pressure fluctuations contain both high-frequency components and low-frequency modulation.

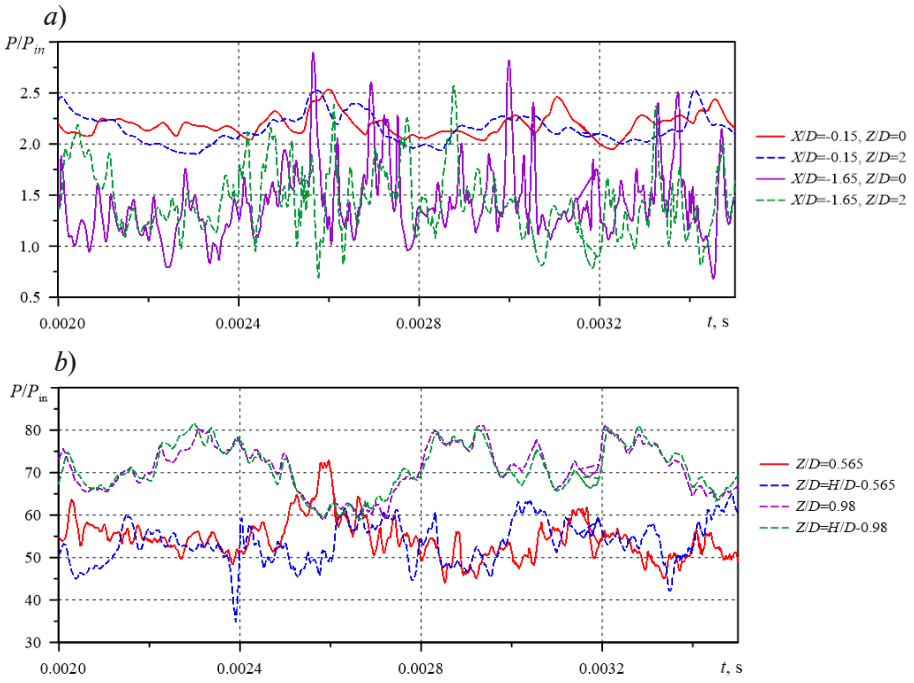


Fig. 10. Time variation of pressure at several points on the surfaces of the plates (*a*) and the leading edge of the body (*b*)

The RMS values of pressure fluctuations, as well as fluctuations of the longitudinal velocity component in front of the body (in the vertical symmetry plane) are shown in Fig. 11; these values are divided by the inlet parameters. Fig. 11,*a* shows a clear pattern of strong oscillations of the bow shock along the direction *X*.

The reason for these oscillations is as follows. Intense velocity fluctuations develop in the separation region in front of the body (see Fig. 11,*b*). The time evolution in the position and intensity of the vortices induces oscillations in the induced oblique compression waves (see Fig. 11,*a*), which in turn leads to bow shock oscillations.

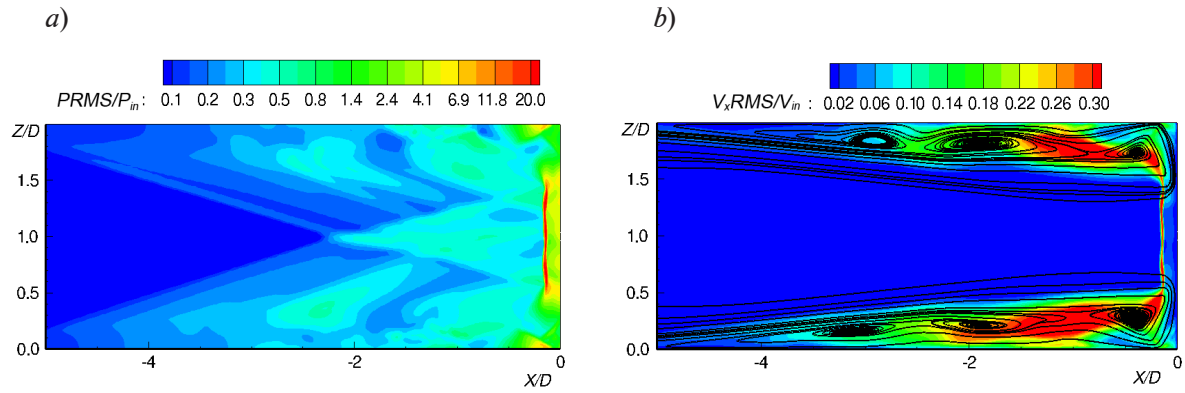


Fig. 11. Fields of RMS pressure fluctuations (*a*) and longitudinal velocity fluctuations (*b*) in vertical symmetry plane in front of the body

## Conclusion

We carried out parametric simulations of supersonic flow around a symmetrical cylindrical body shaped as a fin bounded at the ends by parallel plates. The ratio of the distance between the plates to the blunt fin diameter (geometric parameter $\chi$) was varied in the simulations.

It was established that the flow is steady for the selected values of the freestream parameters in the case of a semi-bounded region ($\chi \to \infty$). The flow structure near the junction is characterized by the presence of an extended separation region in front of the body with a system of horse-shoe-shaped vortices, also accompanied by a bow shock and induced oblique compression waves. If the distance between the plates is sufficiently reduced, first, weakly unsteady flow evolves: small oscillations are observed in the flow only near the junction between the body and the plates; with a further decrease in the distance (the parameter $\chi$ decreases from 3 to 2), the flow pattern becomes significantly nonstationary.

Analysis of time-averaged velocity and pressure fields (always symmetrical with respect to the central plane) indicates that a decrease in the distance between the plates generally leads to a shift of the bow shock closer to the streamlined body and an increase in the thickness of the separation region. When instantaneous flow becomes significantly unsteady, the structure of averaged flow in the separation region undergoes changes: the number of pronounced vortices is smaller, and the separation region is less extensive.

As the distance between the plates decreases, the regions of viscous-inviscid interaction located near the plates increasingly affect the inviscid core of the flow, and then each other. This is clearly manifested in changes in the distribution of pressure and the Stanton number on the surface of the body and plates. In particular, when the parameter $\chi$ decreases, the local maxima of pressure and heat transfer shift to the stagnation point in the center of the body, while the peak values increase significantly.

In the case of significantly unsteady flow simulated for $\chi = 2$, the instantaneous flow fields are not symmetrical with respect to the vertical symmetry plane, and pressure fluctuations contain both high-frequency and low-frequency components. Intense velocity fluctuations are observed in the separation region in front of the body. The time evolution in the position and intensity of the vortices inside the separation region causes fluctuations in the induced oblique compression waves, which, in turn, leads to fluctuations in the bow shock.

Computing resources of the Polytechnic Supercomputer Center (www.scc.spbstu.ru) were used for the simulations.

## REFERENCES

1. **Tutty O. R., Roberts G. T., Schuricht P. H.,** High-speed laminar flow past a fin-body junction, J. Fluid Mech. 737 (25 Dec) (2013)19–55.

2. **Mortazavi M., Knight D**., Simulation of hypersonic-shock-wave–laminar-boundary-layer interaction over blunt fin, AIAA J. 57 (8) (2019) 3506–3523.

3. **Lindцrfer S. A. Combs C. S., Kreth P. A., et al.,** Scaling of cylinder-generated shock-wave/turbulent boundary-layer interactions, Shock Waves. 30 (4) (2020) 395–407.

4. **Knight D., Mortazavi M.,** Hypersonic shock wave transitional boundary layer interactions – A review, Acta Astronaut. 151 (Oct) (2018) 296–317.

5. **Kolesnik E. V., Smirnov E. M., Smirnovsky A. A.,** Numerical solution of a 3D problem on a supersonic viscous gas flow past a plate-cylindrical body junction at M 2.95, St. Petersburg Polytechnical State University Journal. Physics and Mathematics. 12 (2) (2019) 7–22 (in Russian).

6. **Kolesnik E. V., Smirnov E. M.,** Numerical analysis of vortex structures and heat transfer in a supersonic flow past the junction of a blunt-fin body and a plate, Tech. Phys. 65 (2) (2020) 174–181.

7. **Sabnis K., Babinsky H.,** A review of three-dimensional shock wave–boundary-layer interactions, Prog. Aerosp. Sci. 143 (1) (2023) 100953.

8. **Gus'kov O. V., Kopchenov V. I., Lipatov I. I., Ostras V. N.,** Protsessy tormozheniya sverkhzvukovykh techeniy v kanalakh [Processes of supersonic flow deceleration in channels], Fizmatlit Publishing, Moscow, 2008 (in Russian).

9. **Penzin V. I.,** Experimental investigation of separated flows in ducts, Publ. by Central Aerohydrodynamic Institute, Moscow, 2009 (in Russian).

10. **Matsuo K., Miyazato Y., Kim H.-D.,** Shock train and pseudo-shock phenomena in internal gas flows, Prog. Aerosp. Sci. 35 (1) (1999) 33–100.

11. **Gnani F., Zare-Behtash H., Kontis K.,** Pseudo-shock waves and their interactions in high-speed intakes, Prog. Aerosp. Sci. 82 (April) (2016) 36–56.

12. **Bruce P. J. K., Babinsky H., Tartinville B., Hirsch C.,** Corner effect and asymmetry in transonic channel flows, AIAA J. 49 (11) (2011) 2382–2392.

13. **Pizzella M., Warning S., Mcquilling M., et al.,** On the effect of test section aspect ratio for shock wave - boundary layer interactions. Proc. 55th AIAA Aerospace Sciences Meeting, 9–13 Jan, 2017. AIAA, 2017-0535. 9 Jan., Grapevine, Texas, USA, 2017. Vol. 10. Pp. 7586–7603.

14. **Eagle W. E., Driscoll J. F.,** Shock wave–boundary layer interactions in rectangular inlets: three-dimensional separation topology and critical points, J. Fluid Mech. 756 (10 Oct) (2014) 328–353.

## СПИСОК ЛИТЕРАТУРЫ

1. **Tutty O. R., Roberts G. T., Schuricht P. H.** High-speed laminar flow past a fin-body junction // Journal of Fluid Mechanics. 2013. Vol. 737. 25 December. Pp. 19–55.

2. **Mortazavi M., Knight D**. Simulation of hypersonic-shock-wave–laminar-boundary-layer interaction over blunt fin // AIAA (American Institute of Aeronautics and Astronautics) Journal. 2019. Vol. 57. No. 8. Pp. 3506–3523.

3. **Lindцrfer S. A. Combs C. S., Kreth P. A., Bond R. B., Schmisseur J. D.** Scaling of cylinder-generated shock-wave/turbulent boundary-layer interactions // Shock Waves. 2020. Vol. 30. No. 4. Pp. 395–407.

4. **Knight D., Mortazavi M.** Hypersonic shock wave transitional boundary layer interactions – A review // Acta Astronautica. 2018. Vol. 151. October. Pp. 296–317.

5. **Колесник Е. В., Смирнов Е. М., Смирновский А. А.** Численное решение трехмерной задачи обтекания установленного на пластине цилиндрического тела сверхзвуковым потоком вязкого газа при M = 2,95 // Научно-технические ведомости СПбГПУ. Физико-математические науки. 2019. Т. 12. № 2. С. 7–22.

6. **Колесник Е. В., Смирнов Е. М.** Численное исследование вихревых структур и теплообмена при сверхзвуковом обтекании области сопряжения затупленного тела и пластины // Журнал технической физики. 2020. Т. 90. № 2. С. 185–192.

7. **Sabnis K., Babinsky H.** A review of three-dimensional shock wave–boundary-layer interactions // Progress in Aerospace Sciences. 2023. Vol. 143. No. 1. P. 100953.

8. **Гуськов О. В., Копченов В. И., Липатов И. И., Острась В. Н.** Процессы торможения сверхзвуковых течений в каналах. М.: Физматлит, 2008. 163 с.

9. **Пензин В. И.** Экспериментальное исследование отрывных течений в каналах. М.: Изд-во Центрального аэрогидродинамического института (ЦАГИ), 2009. 280 с.

10. **Matsuo K., Miyazato Y., Kim H.-D.** Shock train and pseudo-shock phenomena in internal gas flows // Progress in Aerospace Sciences. 1999. Vol. 35. No. 1. Pp. 33–100.

11. **Gnani F., Zare-Behtash H., Kontis K.** Pseudo-shock waves and their interactions in high-speed intakes // Progress in Aerospace Science. 2016. Vol. 82. April. Pp. 36–56.

12. **Bruce P. J. K., Babinsky H., Tartinville B., Hirsch C.** Corner effect and asymmetry in transonic channel flows // AIAA Journal. 2011. Vol. 49. No. 11. Pp. 2382–2392.

13. **Pizzella M., Warning S., Mcquilling M., Purkey A., Scharnhorst R., Mani M., Benek J, Suchyta C., Babinsky H.** On the effect of test section aspect ratio for shock wave - boundary layer interactions // Proceedings of the 55th AIAA Aerospace Sciences Meeting. 9–13 January, 2017. Grapevine, Texas, USA: AIAA, 2017-0535. 9 January, 2017. Vol. 10. Pp. 7586–7603.

14. **Eagle W. E., Driscoll J. F.** Shock wave–boundary layer interactions in rectangular inlets: three-dimensional separation topology and critical points // Journal of Fluid Mechanics. 2014. Vol. 756. 10 October. Pp. 328–353.

## THE AUTHORS

**KOLESNIK Elizaveta V.**
*Peter the Great St. Petersburg Polytechnic University*
29 Politechnicheskaya St., St. Petersburg, 195251, Russia
kolesnik_ev@mail.ru
ORCID: 0000-0002-6308-733X

**BABICH Elena V.**
*Peter the Great St. Petersburg Polytechnic University*
29 Politechnicheskaya St., St. Petersburg, 195251, Russia
lll.helen.lll@mail.ru
ORCID: 0000-0003-1442-4886

**SMIRNOV Evgeny M.**
*Peter the Great St. Petersburg Polytechnic University*
29 Politechnicheskaya St., St. Petersburg, 195251, Russia
smirnov_em@spbstu.ru
ORCID: 0000-0002-7218-6372

## СВЕДЕНИЯ ОБ АВТОРАХ

**КОЛЕСНИК Елизавета Владимировна** – *кандидат физико-математических наук, доцент Высшей школы прикладной математики и вычислительной физики Санкт-Петербургского политехнического университета Петра Великого.*
195251, Россия, г. Санкт-Петербург, Политехническая ул., 29
kolesnik_ev@mail.ru
ORCID: 0000-0002-6308-733X

**БАБИЧ Елена Викторовна** – *студентка Физико-механического института Санкт-Петербургского политехнического университета Петра Великого.*
195251, Россия, г. Санкт-Петербург, Политехническая ул., 29
lll.helen.lll@mail.ru
ORCID: 0000-0003-1442-4886

**СМИРНОВ Евгений Михайлович** – *доктор физико-математических наук, профессор Высшей школы прикладной математики и вычислительной физики Санкт-Петербургского политехнического университета Петра Великого.*

195251, Россия, г. Санкт-Петербург, Политехническая ул., 29

smirnov_em@spbstu.ru

ORCID: 0000-0002-7218-6372

*Received 19.07.2024. Approved after reviewing 26.07.2024. Accepted 26.07.2024.*

*Статья поступила в редакцию 19.07.2024. Одобрена после рецензирования 26.07.2024. Принята 26.07.2024.*